This is to certify that the
thesis entitled

AN IMPROVED FINITE DIFFERENCE METHOD FOR SOLVING COMPLEX GROUNDWATER FLOW PROBLEMS IN GENERAL 2-D ANISOTROPIC MEDIA

presented by

SOHEIL AFSHARI

has been accepted towards fulfillment
of the requirements for the

Master of Science	degree in	Department of Civil and Environmental Engineering

Major Professor's Signature

12/2/2003

Date

AN IMPROVED FINITE DIFFERENCE METHOD FOR SOLVING COMPLEX GROUNDWATER FLOW PROBLEMS IN GENERAL 2-D ANISOTROPIC MEDIA

By

Soheil Afshari

A THESIS

Submitted to
Michigan State University
in partial fulfillment of the requirements
for the degree of

MASTER OF SCIENCE

Department of Civil and Environmental Engineering

2003

ABSTRACT

AN IMPROVED FINITE DIFFERENCE METHOD FOR SOLVING COMPLEX GROUNDWATER FLOW PROBLEMS IN GENERAL 2-D ANISOTROPIC MEDIA

By

Soheil Afshari

In this thesis, we present an improved finite difference (FD) method for solving complex 2-D groundwater flow problems in anisotropic media. In particular, we address one of the major difficulties in solving the tensorial form of the groundwater flow equation. Traditional FD techniques, when applied to the flow equation containing the complete conductivity tensor, often lead to physically unrealistic results. Traditional FD methods are particularly problematic when the anisotropy is strong and its major orientation deviates significantly from the rectilinear coordinate system. Our new approach eliminates the problem by approximating the tensorial "diffusion" terms in a rotated coordinate system locally aligned with the major direction of anisotropy. It then expresses and interpolates the non-nodal heads in the resulting numerical expression in terms of global nodal heads. The result is a significantly improved scheme that is more accurate and robust than the traditional finite difference scheme. In addition, the new approach is monotonic and always leads to a physically meaningful solution. We demonstrate the advantage of the improved FD approach with a number of groundwater flow examples and a systematic comparison with exact solutions and solutions obtained from traditional FD methods.

ACKNOWLEDGEMENTS

I gratefully acknowledge the contribution of those who have made this thesis possible. My deepest gratitude goes to Dr. Shu-Guang Li, Associate Professor, Department of Civil and Environmental Engineering, Michigan State University, my thesis director and my advisor during my course work. I appreciate his fatherly advice, patience, and continual encouragement throughout my entire graduate program.

I also wish to extend my appreciation to Dr. Roger B. Wallace, Associate Professor, Department of Civil and Environmental Engineering; Dr. Susan Masten, Professor, Department of Civil and Environmental Engineering, Michigan State University; and Dr. David C Wiggert, Professor, Department of Civil and Environmental Engineering, Michigan State University, for serving in my thesis committee and for valuable comments in this study.

Also, I wish to thank Dr. H.S. Liao for implementing the Fortran code for improved FD method in Interactive Groundwater Model (IGW); and Dr. Qun Liu for his patience and restless help during my simulation study.

Research funding was obtained from National Science Foundation (NSF).

Finally, I want to thank my family, especially my parents and my uncle Dr. Sirous Haji-Djafari for their love, care, support and understanding.

TABLE OF CONTENTS

List of Figures

List of Tables

1 Introduction

This thesis aims at developing, documenting, and demonstrating an improved finite-difference (FD) method for solving complex 2-D groundwater flow problems in anisotropic media. In particular, the thesis addresses one of the major difficulties in solving the groundwater flow equation when the aquifer is strongly anisotropic and the major orientation of anisotropy deviates significantly from the rectilinear coordinate system.

1.1 Geological Background

In some specific geological formations like sloping aquifers, fluvial channel deposits, glacial deposits, or secondary permeability terrains and fractured rocks, anisotropy expresses with orientation. In many cases, this orientation varies from point to point and from layer to layer. Under such situations, traditional FD techniques become problematic and lead to non-meaningful or physically unrealistic results.

1.1.1 Sloping aquifers

One of the common examples of anisotropic formations with a variable orientation is a sloping aquifer system. Figure 1 represents a system of dipping hydrostratigraphic units hydraulically connected with a shallow unconfined aquifer.

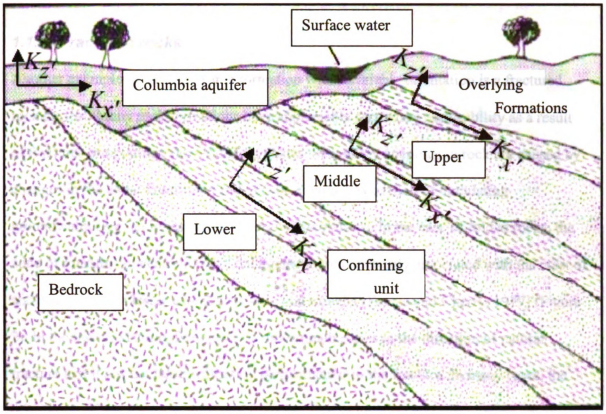

Figure 1. A sloping aquifer system [modified from M. P. Anderson and W. W. Woessner, 1992].

While the water in the unconfined unconsolidated aquifer tends to move in the horizontal direction, it has a natural tendency to flow at an angle along the dipping layers in the confined aquifer system. In this case, the preferential flow is oriented in two different directions and, obviously, it is impossible to align both simultaneously with the overall model grid axes.

1.1.2 Fractured rocks

Another example of an anisotropic formation with a variable orientation is a fractured rock system. Many rock formations have appreciable secondary permeability as a result of fractures or openings along bedding planes. Secondary openings in rock are caused by changes in the stress conditions and may be enlarged as a result of circulating groundwater (e.g., in limestone or dolomite dissolution). In the case of folded rocks, the zone of fracture concentration and enlargement are commonly associated with the crest of anticlines and to a lesser extent with synclinal troughs [Freeze and Cherry, 1979] (Figure 2). In the fractured zone, flow tends to move much easier in the direction of natural fracture and it has the least infiltration perpendicular to the fracture. In many cases, the orientation of the fractures may vary from location to location and from formation to formation. It may also likely be different from the orientation in the overlying unconsolidated aquifers since it is created by a different mechanism.

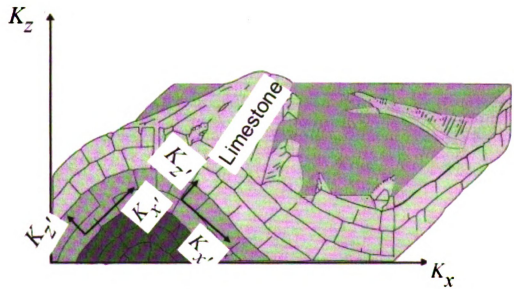

Figure 2. Fractured carbonate rock [modified from Freeze and Cherry, 1979].

1.1.3 Fluvial channel deposits

Fluvial deposits are additional example that often exhibits anisotropy with variable orientation. The fluvial deposits are the materials laid down by deposition in river channels or on flood plains. Fluvial materials occur in nearly all regions. Figure 3 illustrates the morphology and variations in deposits formed by meandering rivers. Because of the way they are deposited and the ever-changing depositional velocities, river deposits have characteristic textural variability that causes much heterogeneity in the distribution of hydraulic properties [Freeze and Cherry, 1979]. These heterogeneous deposits are frequently stratified and oriented along the streams. When the average properties of large volumes are considered, the heterogeneous character of fluvial deposits imparts a strong anisotropy to the system and creates preferential flow parallel to the stream. Obviously, the major orientation of anisotropy varies as the channel winds around and shifts in its position [Freeze and Cherry, 1979].

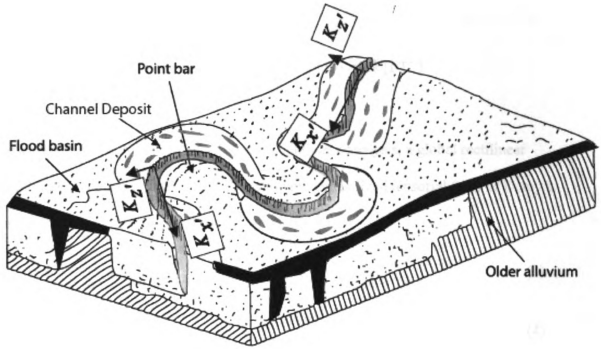

Figure 3. Fluvial channel deposit [modified from Freeze and Cherry, 1979].

1.2 Darcy's Law in General Anisotropic Media

Under these situations, Darcy's law applies only locally along the 'principal' directions or the preferential flow direction and the direction normal to it. If the local principal coordinates are denoted as x', z' (see Figure 4), Darcy's equation can be written as:

$$q_{x'} = -K_{x'} \frac{\partial \Phi}{\partial x'} \tag{1}$$

$$q_{z'} = -K_{z'} \frac{\partial \Phi}{\partial z'} \tag{2}$$

where,

$q_{x'}, q_{z'}$ the specific discharge x' and z' respectively [LT^{-1}]

x', z' the local coordinate system [L]

Φ the hydraulic head [L]

$K_{x'}$, and $K_{z'}$ the principal hydraulic conductivities [LT^{-1}]

However, in a system wide finite-difference modeling analysis, a global rectilinear coordinate is required. In this case, the following generalized tensorial form of Darcy's law must be used (Eqs. 3 and 4):

$$q_x = -K_{xx}\frac{\partial \Phi}{\partial x} - K_{xz}\frac{\partial \Phi}{\partial z} \tag{3}$$

$$q_z = -K_{zx}\frac{\partial \Phi}{\partial x} - K_{zz}\frac{\partial \Phi}{\partial z} \tag{4}$$

where,

x and z the spatial coordinates in the global rectilinear system[L]

q_x and q_z the specific discharges along x and z respectively in the global coordinate system [LT^{-1}]

K_{xx}, K_{xz}, K_{zx}, and K_{zz} components of the hydraulic conductivity tensor which represent an anisotropic medium [LT^{-1}].

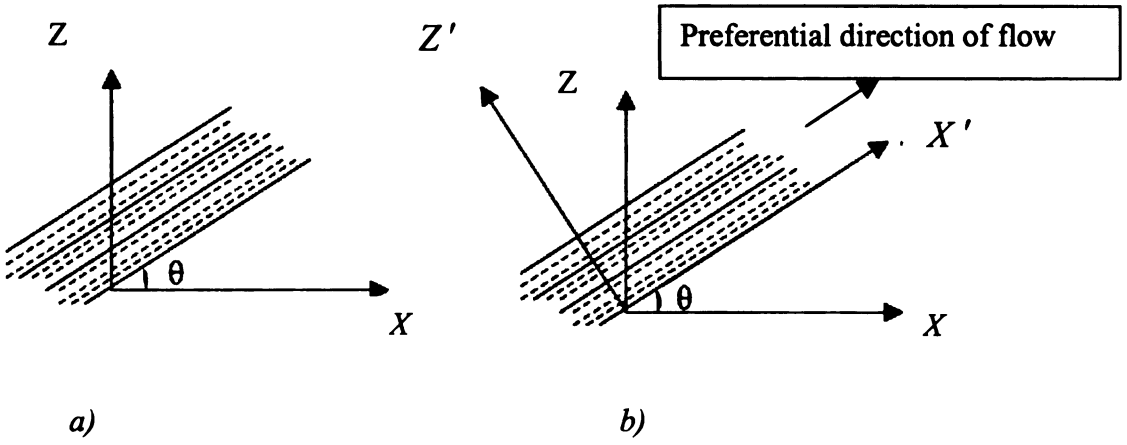

Figure 4. (a) a global coordinate system and (b) a local coordinate system aligned with the bedding (the dashed lines represents bedding orientation) [modified from Wang, H.F. and Anderson, M.P., 1982].

The cross-conductivity K_{xz} represents the x-seepage flow induced by a unit hydraulic gradient in the z direction. For instance, the term $K_{xz}\frac{\partial \Phi}{\partial z}$ in Eq. (3) reflects the fact that a head gradient in one direction (e.g., the z direction) will induce some flow along the beds, and hence there will be a component of flow in the other direction (e.g., the x direction). Note that the principal conductivities and the orientation are the fundamental properties that characterize an aquifer formation and the conductivity tensor is a derived property and can be related to the principal conductivities and the orientation. In the case of two dimensional (2-D) flow in the xz plane, this relationship is given by the following equations:

$$\begin{bmatrix} K_{xx} & K_{xz} \\ K_{zx} & K_{zz} \end{bmatrix} = R^{-1} \begin{bmatrix} K_{x'} & 0 \\ 0 & K_{z'} \end{bmatrix} R \tag{5}$$

with

$$R^{-1} = \begin{bmatrix} \cos\theta & -\sin\theta \\ \sin\theta & \cos\theta \end{bmatrix} \tag{6}$$

where

R the rotation matrix

R^{-1} the inverse of R

θ the angle of anisotropy, which is measured from the x axes of global direction [degree] in the counterclockwise direction.

1.3 Governing Equation For 2-D Anisotropic Flow

To systematically analyze groundwater flow using Eq. (3), and (4) we must first know the hydraulic head distribution. An equation for determining the hydraulic head can be obtained from the mass conservation equation:

$$S_s \frac{\partial \Phi}{\partial t} = \frac{\partial q_x}{\partial x} + \frac{\partial q_z}{\partial z} + r \tag{7}$$

where

S_s specific storage, [-]

r a source/sink related term, [L/T]

t time, [T].

Substituting Eqs. (3) and (4) into Eq. (7) we obtain the following equation

$$S_s \frac{\partial \Phi}{\partial t} = \frac{\partial}{\partial x}\left(K_{xx} \frac{\partial \Phi}{\partial x}\right) + \frac{\partial}{\partial x}\left(K_{xz} \frac{\partial \Phi}{\partial z}\right) + \frac{\partial}{\partial z}\left(K_{zz} \frac{\partial \Phi}{\partial z}\right) + \frac{\partial}{\partial z}\left(K_{zx} \frac{\partial \Phi}{\partial x}\right) + r \quad (8)$$

Eq. (8) describes groundwater flow in a 2-D anisotropic and heterogeneous media. For illustration purpose, we assume that the media is homogeneous (e.g., the hydraulic conductivity is independent of distance).

2 Previous Research

Except for certain special situations under highly restrictive assumptions Eq. (8) must be solved on a computer using grid-based numerical methods such as a finite difference (FD) or a finite element (FE) method.

Historically orientation in anisotropy has been accounted for only in finite element models using unstructured grids. For example, the commonly used finite-element code FEMWATER [Lin and others, 2001], the newest version of SUTRA [Voss and Provost, 2002], and FEHM [Dash and others, 2002] allow mutually orthogonal anisotropy directions to be in any orientation. In most finite difference models, the effects of the cross-conductivity terms are ignored, implicitly assuming that horizontal anisotropy is unimportant and the aquifer layers are always oriented approximately horizontal. For example, the popular MODFLOW-2000 [Harbaugh and others,2000] with either the Layer-Property Flow (LPF) Package [Harbaugh and others, 2000] or the Hydrogeologic-Unit Flow (HUF) Package [Anderman and Hill, 2000] have been limited to grid-direction anisotropy. That is, the simulated direction of anisotropy has been limited to being oriented along the grid axis [USGS open file report 02-409, Anderman E. R. et al., 2002].

Most recently, some FD models such as VST2D [Friedel, 2001] have taken into account the orientation in anisotropy. However, as we will explain in the following subsection, these extended FD models, being unable to approximate accurately the cross-conductivity terms, lead frequently to ill-conditioned matrices and significant errors in the magnitude and direction of predicted flow, especially for large and complex flow systems.

2.1 Traditional FD approach

In this section, we review the traditional finite difference method for solving general anisotropic flow problems. We further examine the source of the numerical difficulty and lay the foundation for the development of an improved methodology.

2.1.1 Transient flow

Most traditional FD methods approximate Eq. (8) by invoking a standard finite difference approximation. Specifically, the time derivative $\frac{\partial \Phi}{\partial t}$ at each nodal point is approximated as follow using the following implicit finite difference:

$$\frac{\partial \Phi}{\partial t} \cong \frac{\Phi_C^{n+1} - \Phi_C^n}{\Delta t} \tag{9}$$

where,

Δt	the length of the time step. [T]
n, n+1	the superscripts are the time index, [-].
Φ_C^{n+1} and Φ_C^n	the head in the center cell respectively at time *(n+1)* and *(n)*, [L].

The spatial derivatives are approximated based on centered finite difference using the following Eq. (10) and (11) (Figure 5 represents the finite difference grid with the index numbering convention).

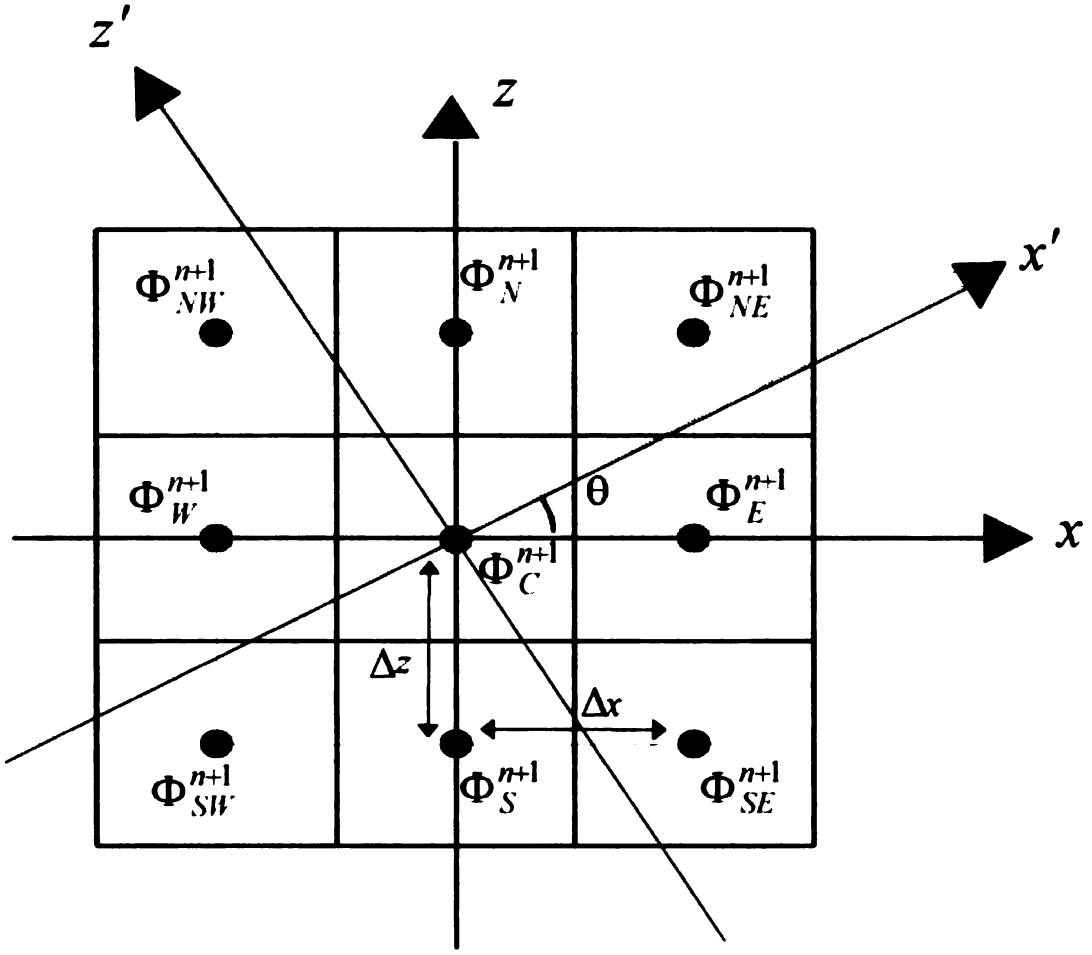

Figure 5. Finite difference grid showing index numbering convention.

For illustration purpose we assume that the media is homogeneous.

$$\frac{\partial}{\partial x}\left(K_{xx}\frac{\partial \Phi^{n+1}}{\partial x}\right) \cong K_{xx}\frac{\Phi_W^{n+1} - 2\Phi_C^{n+1} + \Phi_E^{n+1}}{(\Delta x)^2} \tag{10}$$

$$\frac{\partial}{\partial x}\left(K_{xz}\frac{\partial \Phi^{n+1}}{\partial z}\right) \cong K_{xz}\frac{\Phi_{NE}^{n+1} - \Phi_{SE}^{n+1} - \Phi_{NW}^{n+1} + \Phi_{SW}^{n+1}}{4\Delta x\,\Delta z} \tag{11}$$

where,

Φ_C^{n+1} the hydraulic head at the center cell at time $n+1$,[L]

$\Phi_N^{n+1}, \Phi_S^{n+1}, \Phi_E^{n+1}, \Phi_W^{n+1}$ the hydraulic heads at the neighboring cells at time $n+1$, [L]

$\Delta x, \Delta z$ grid spacing in x and z direction, [L]

Other spatial derivative terms of the general Eq. (8) can be approximated in a similar fashion.

By substituting the finite-difference approximation Eqs. (9) through (11) into Eq. (8) and reorganizing, one obtains the equation:

$$\Phi_C^{n+1} = a_N \Phi_N^{n+1} + a_S \Phi_S^{n+1} + a_E \Phi_E^{n+1} + a_W \Phi_W^{n+1} + a_{NW} \Phi_{NW}^{n+1} + \\ + a_{NE} \Phi_{NE}^{n+1} + a_{SW} \Phi_{SW}^{n+1} + a_{SE} \Phi_{SE}^{n+1} + b\Phi_C^n + s \qquad (12)$$

where,

$\Phi_N^{n+1}, \Phi_S^{n+1}, \Phi_E^{n+1}, \Phi_W^{n+1}, \Phi_{NE}^{n+1}, \Phi_{NW}^{n+1}, \Phi_{SE}^{n+1}, \Phi_{SW}^{n+1}$ the hydraulic heads in the neighboring cells at time $n+1$, [L]

s a term related to general sink/source term, [L]

The symbols $a_N, a_S, a_E, a_W, a_{NE}, a_{NW}, a_{SE}, a_{SW}, b$ are weighting coefficients given by:

$$a_N = a_S = 2A\Delta x^2\left(K_x, \sin^2\theta + K_z, \cos^2\theta\right) \tag{13}$$

$$a_E = a_W = 2A\Delta z^2\left(K_z, \sin^2\theta + K_x, \cos^2\theta\right) \tag{14}$$

$$a_{NW} = a_{SE} = \frac{-A}{2}\Delta x\,\Delta z\,(K_x, -K_z,)\sin 2\theta \tag{15}$$

$$a_{NE} = a_{SW} = \frac{A}{2}\Delta x\,\Delta z\,(K_x, -K_z,)\sin 2\theta \tag{16}$$

$$b = 2AS_S\frac{\Delta x^2\Delta z^2}{\Delta t} \tag{17}$$

$$s = 2Ar\Delta x^2\Delta z^2 \tag{18}$$

where,

$$A = \frac{0.5\Delta t}{\left(\Delta x^2 K_x, \sin^2\theta + \Delta x^2 K_z, \cos^2\theta + \Delta z^2 K_x, \cos^2\theta + \Delta x^2 K_z, \sin^2\theta\right)2\Delta t + S_s\Delta x^2\Delta z^2} \tag{19}$$

Equation (12) provides a discrete representation of the governing flow equation. It is a discrete mathematical statement of the mass balance for a cell over a time interval t^n to t^{n+1}.

2.1.2 Steady state flow

In the case of steady state flow, the numerical representation can be further simplified. This can be obtained by simply letting S_s be zero in Eq. (13) through Eq. (18). The result is the following FD scheme:

$$\Phi_C = a_N \Phi_N + a_S \Phi_S + a_E \Phi_E + a_W \Phi_W + a_{NW} \Phi_{NW} + a_{NE} \Phi_{NE} + a_{SW} \Phi_{SW} + a_{SE} \Phi_{SE} + s \tag{20}$$

with the coefficients given by:

$$a_N = a_S = 2A\Delta x^2 \left(K_x, \sin^2\theta + K_z, \cos^2\theta\right) \tag{21}$$

$$a_E = a_W = 2A\Delta z^2 \left(K_z, \sin^2\theta + K_x, \cos^2\theta\right) \tag{22}$$

$$a_{NW} = a_{SE} = \frac{-A}{2}\Delta x\,\Delta z\,(K_x, -K_z,)\sin 2\theta \tag{23}$$

$$a_{NE} = a_{SW} = \frac{A}{2}\Delta x\,\Delta z\,(K_x, -K_z,)\sin 2\theta \tag{24}$$

$$s = 2Ar\Delta x^2 \Delta z^2 \tag{25}$$

where

$$A = \frac{1}{4(\Delta z^2 K_x, \cos^2\theta + \Delta x^2 K_x, \sin^2\theta + \Delta x^2 K_z, \cos^2\theta + \Delta z^2 K_z, \sin^2\theta)} \tag{26}$$

Equation (12) or (20) indicates that the central head in a cell can be expressed as the weighted average of the heads in the surrounding cells. The weighting coefficients dictate the performance of the numerical scheme. These coefficients are a function of orientation and the ratio of anisotropy, as well as, time step and grid spacing.

A basic physical principal requires that these weighting coefficients be positive. However, when the off-diagonal components of the hydraulic conductivity tensor are not zero, the weighting coefficients derived from traditional FD methods may not satisfy this positivity requirement. In fact, as long as the angle of anisotropy (θ) is nonzero, the corner weighting coefficients (a_{NE},a_{SW} or a_{NW},a_{SE}) depending on angle of anisotropy for the central head are always negative. The coefficients become more negative as the orientation of anisotropy and the ratio of anisotropy increases. The magnitude of the negative coefficients are largest when the orientation is diagonal (e.g., close to 45°). In other words, the head in the center cell would decrease in response to an increase in the head in the north-west (*NW*) and south-east (*SE*) cells. This is not meaningful and it is the source of numerical problems encountered in the traditional FD methods.

2.2 The MODFLOW approach

2.2.1 Transient flow

The popular USGS MODFLOW [MODFLOW-2000, Harbaugh and others,2000] program circumvents the numerical problem by ignoring the orientation of anisotropy. In particular, MODFLOW neglects the off-diagonal component of the hydraulic conductivity tensor (assume $\theta = 0^{\circ}$), and always works with the following flow equations (the 2-D flow *xz* scenario):

$$S_s \frac{\partial \Phi}{\partial t} = \frac{\partial}{\partial x}\left(K_{xx} \frac{\partial \Phi}{\partial x} \right) + \frac{\partial}{\partial z}\left(K_{zz} \frac{\partial \Phi}{\partial z} \right) + r \tag{27}$$

With the application of the standard implicit finite difference over time and central finite difference in space, one obtains the same general numerical scheme in Eq. (12) with the following weighting coefficients:

$$a_N = a_S = 2A\Delta x^2 K_z, \tag{28}$$

$$a_E = a_W = 2A\Delta z^2 K_x, \tag{29}$$

$$a_{NE} = a_{NW} = a_{SE} = a_{SW} = 0 \tag{30}$$

$$b = 2AS_S \frac{\Delta x^2 \Delta z^2}{\Delta t} \tag{31}$$

$$s = 2Ar\Delta x^2 \Delta z^2 \tag{32}$$

where,

$$A = \frac{\Delta t}{2\left[\left(\Delta x^2 K_{z'} + \Delta z^2 K_{x'}\right) 2\Delta t + S_s \Delta x^2 \Delta z^2\right]} \tag{33}$$

2.2.2 Steady state flow

In the case of steady state flow, the weighting coefficients can be further simplified by assuming S_s equal to zero in Eqs. (28) through (32) the result is:

$$a_N = a_S = A K_{z'} \Delta x^2 \tag{34}$$

$$a_E = a_W = A K_{x'} \Delta z^2 \tag{35}$$

$$a_{NE} = a_{NW} = a_{SE} = a_{SW} = 0 \tag{36}$$

$$s = A r \Delta x^2 \Delta z^2 \tag{37}$$

where

$$A = \frac{0.5}{\Delta x^2 K_{z'} + \Delta z^2 K_{x'}} \tag{38}$$

Although the weighting coefficients associated with MODFLOW are all positive and symmetric, the corner information is not used. Not surprisingly, the distribution of the weighting coefficients does not properly reflect the impact of the orientation in anisotropy.

3 Improved FD approach

3.1 Transient flow

In this section, we present an improved FD approach for modeling groundwater flow in general 2-D anisotropic media. Recognizing the numerical difficulty associated with the cross-conductivity terms, we work with the following governing equation that is free of the K_{xz}, K_{zx} terms:

$$S_s \frac{\partial \Phi}{\partial t} = \frac{\partial}{\partial x'}\left(K_{x'} \frac{\partial \Phi}{\partial x'}\right) + \frac{\partial}{\partial z'}\left(K_{z'} \frac{\partial \Phi}{\partial z'}\right) + r \tag{39}$$

We are able to eliminate the "trouble making" cross-conductivity terms, because the equation is written in a rotated coordinate system locally aligned with the major direction of anisotropy. We further invoke implicit finite differencing over time (Eq. 12) as in a standard FD method and the following central differencing for the spatial terms in the local x', z' system:

$$\frac{\partial}{\partial x'}\left(K_{x'} \frac{\partial \Phi^{n+1}}{\partial x'}\right) \cong K_{x'} \frac{\Phi'^{n+1}_W - 2\Phi^{n+1}_C + \Phi'^{n+1}_E}{(\Delta x')^2} \tag{40}$$

$$\frac{\partial}{\partial z'}\left(K_{z'} \frac{\partial \Phi^{n+1}}{\partial z'}\right) \cong K_{z'} \frac{\Phi'^{n+1}_N - 2\Phi^{n+1}_C + \Phi'^{n+1}_S}{(\Delta z')^2} \tag{41}$$

where,

$K_{x'}, K_{z'}$ the principal hydraulic conductivities, [LT^{-1}].

$\Delta x', \Delta z'$ the grid spacing in x' and z' direction, [L].

$\Phi'^{n+1}_N, \Phi'^{n+1}_S, \Phi'^{n+1}_E$, and Φ'^{n+1}_W the non-nodal heads in the rotated coordinate system, [L] as shown in Figure 6.

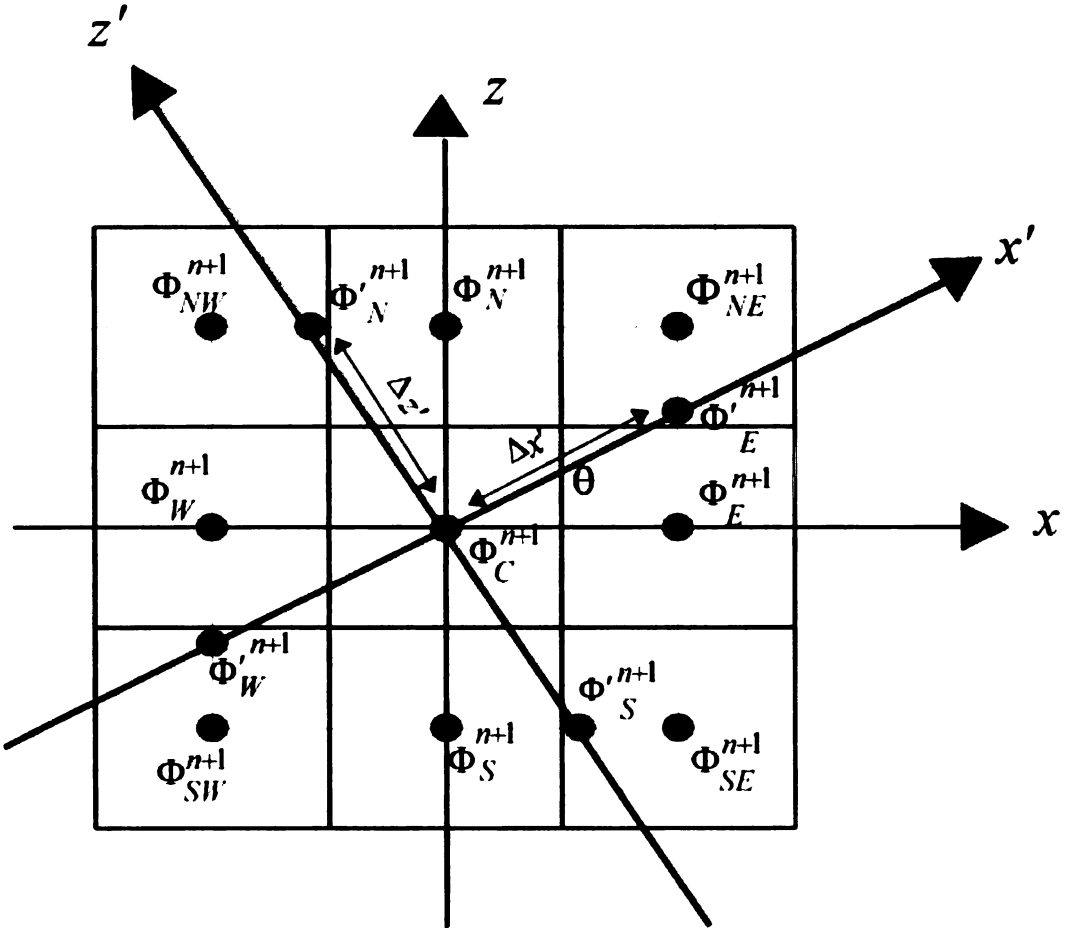

Figure 6. Nodal and non-nodal head values.

Substituting Eqs. (9), (40), and (41) in Eq. (39), we obtain the following:

$$\Phi_C^{n+1} = 2A(K_z,\Delta x'^2\Phi_N'^{n+1} + K_z,\Delta x'^2\Phi_S'^{n+1} + K_x,\Delta z'^2\Phi_E'^{n+1} + K_x,\Delta z'^2\Phi_W'^{n+1} + \frac{\Delta x'^2\Delta z'^2 \cdot S_s}{\Delta t}\Phi_C^n + r\Delta x'^2\Delta z'^2) \tag{42}$$

where,

$$A = \frac{0.5\Delta t}{2\left(\Delta x'^2 K_z, + \Delta z'^2 K_x,\right)\Delta t + S_s\Delta x'^2\Delta z'^2} \tag{43}$$

Note that Eq. (42) cannot be directly used yet since the central head is expressed in terms of the non-nodal heads. They must be related to the nodal heads before the equation can be used in an overall numerical analysis. This can be achieved in a straightforward fashion using the following basic linear interpolations based on the nearest nodal heads

$$\Phi_N'^{n+1} = \tan\theta\frac{\Delta z}{\Delta x}(\Phi_{NW}^{n+1} - \Phi_N^{n+1}) + \Phi_N^{n+1} \tag{44}$$

$$\Phi_S'^{n+1} = \tan\theta\frac{\Delta z}{\Delta x}(\Phi_{SE}^{n+1} - \Phi_S^{n+1}) + \Phi_S^{n+1} \tag{45}$$

$$\Phi_W'^{n+1} = \tan\theta\frac{\Delta x}{\Delta z}(\Phi_{SW}^{n+1} - \Phi_W^{n+1}) + \Phi_W^{n+1} \tag{46}$$

$$\Phi_E'^{n+1} = \tan\theta\frac{\Delta x}{\Delta z}(\Phi_{NE}^{n+1} - \Phi_N^{n+1}) + \Phi_E^{n+1} \tag{47}$$

Substituting the Eqs. (44) through (47) into Eq. (42) produces the same numerical scheme as in Eq (12) with the following different weighting coefficients. These coefficients are for the case of $0° \le \theta < 45°$:

$$a_N = a_S = BK_z,\Delta x\left(\Delta x - \Delta z \tan\theta\right) \tag{48}$$

$$a_E = a_W = BK_x,\Delta z\left(\Delta z - \Delta x \tan\theta\right) \tag{49}$$

$$a_{NW} = a_{SE} = BK_z,\Delta x\,\Delta z \tan\theta \tag{50}$$

$$a_{NE} = a_{SW} = BK_x,\Delta x\,\Delta z \tan\theta \tag{51}$$

$$b = BS_S \frac{\Delta x^2 \Delta z^2}{\Delta t \cos^2\theta} \tag{52}$$

$$s = \frac{Br\Delta x^2 \Delta z^2}{\cos^2\theta} \tag{53}$$

where,

$$B = \frac{1}{2K_x,\Delta z^2 + 2K_z,\Delta x^2 + \dfrac{S_s \Delta x^2 \Delta z^2}{\cos^2\theta \Delta t}} \tag{54}$$

Similarly the coefficients could be obtained for other angles (θ's). Simply we have to apply different interpolation equations for each sector of 45 degrees.

3.2 Steady state flow

In the case of steady state flow, Eq.(42) reduces to

$$\Phi_C^{n+1} = B(K_z,\Delta x'^2\Phi_N'^{n+1} + K_z,\Delta x'^2\Phi_S'^{n+1} + K_x,\Delta z'^2\Phi_E'^{n+1} + K_x,\Delta z'^2\Phi_W'^{n+1} + r\Delta x'^2\Delta z'^2) \tag{55}$$

where,

$$B = \frac{1}{2\left(\Delta x'^2 K_z, + \Delta z'^2 K_x,\right)} \tag{56}$$

which is obtained from Eq. (42) by setting S_s to zero. By substituting the same interpolation equations in to Eq. (55), we obtain a steady state scheme or Eq. (20) with the following coefficients:

$$a_N = a_S = BK_z,\Delta x\left(\Delta x - \Delta z\tan\theta\right) \tag{57}$$

$$a_E = a_W = BK_x,\Delta z\left(\Delta z - \Delta x\tan\theta\right) \tag{58}$$

$$a_{NW} = a_{SE} = BK_z,\Delta x\,\Delta z\tan\theta \tag{59}$$

$$a_{NE} = a_{SW} = BK_x,\Delta x\,\Delta z\tan\theta \tag{60}$$

where,

$$B = \frac{0.5}{K_x,\Delta z^2 + K_z,\Delta x^2} \tag{61}$$

Notice that all weighting coefficients obtained from improved FD approach, for any given anisotropy direction, are positive. Also note how the weighting coefficients vary proportional to the natural direction of anisotropy. As expected, the center head is always influenced more by surrounding heads along the direction of orientation than those across.

As we will demonstrate in the next section, the improved FD method is significantly more accurate. In addition, the new scheme is more robust than the traditional FD scheme and always leads to a physically meaningful solution.

4 Illustrative Examples

In this section, we demonstrate the advantage of the improved FD method with two specific examples and a systematic comparison with exact solution, when available, and the solutions obtained using the traditional FD methods.

4.1 A Simple Example

Our first example considers a simple groundwater problem that involves steady state uniform flow driven by a constant horizontal gradient in a 2-D homogeneous, anisotropic media with the major direction of anisotropy oriented at 30° with the horizontal axis (Figure 7). The top and bottom boundary conditions are imposed in such a way that flow is uniform throughout the solution domain (Figure 7).

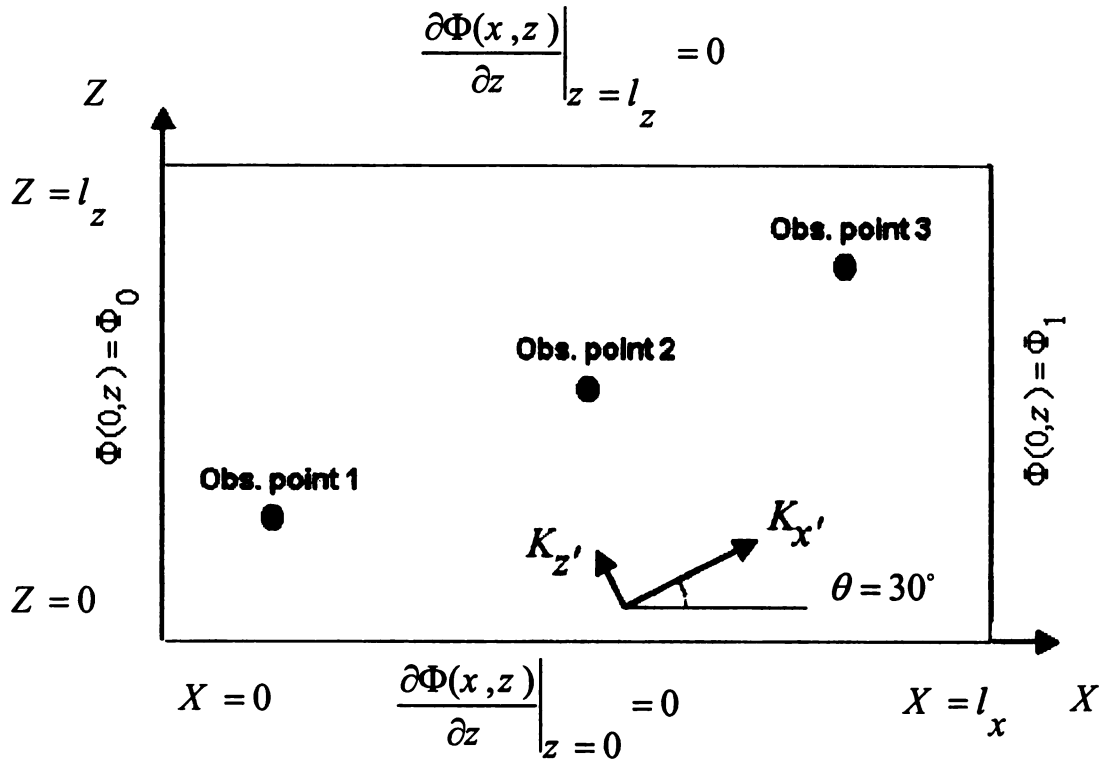

Figure 7. Definition sketch for the simple example

In this case, the problem has the following exact solution:

$$\Phi(x,z) = \Phi_0 + \frac{\Phi_1 - \Phi_0}{l_x} x \tag{62}$$

$$v_x(x,z) = \frac{-K_{xx}}{n}\left(\frac{\Phi(x,z) - \Phi_0}{x}\right) \tag{63}$$

$$v_z(x,z) = \frac{-K_{xz}}{n}\left(\frac{\Phi(x,z) - \Phi_0}{x}\right) \tag{64}$$

where,

Φ_0, Φ_1	the prescribed head on the left and right boundaries, respectively [L].
x, z	the horizontal and vertical spatial coordinate measured from the left constant head boundaries and down impermeable boundary, [L]
l_x	the length of the domain in the x direction [L]
l_z	the length of the domain in the z direction [L]
n	porosity [-]
v_x, v_z	the average linear velocities in x and z direction [LT^{-1}]

We solved the problem numerically using the traditional FD method, improved FD method, and the MODFLOW method based on the following parameters and inputs:

Table 1. Input physical and numerical parameters for the simple example

Parameter	Value (unit)
θ	*30°*
Φ_0	*10 (m)*
Φ_1	*2 (m)*
l_x	*800 (m)*
l_z	*600 (m)*
K_x'	*50 (m/day)*
K_z'	*5 (m/day)*
n	*0.3 (-)*
Δx	*5 (m)*
Δz	*5 (m)*

The results are summarized graphically in Figures 8 through 11. Obtained solutions for each method are achieved by utilizing the Interactive Groundwater Model (IGW) [Shu-Guang Li, et al, 2002].

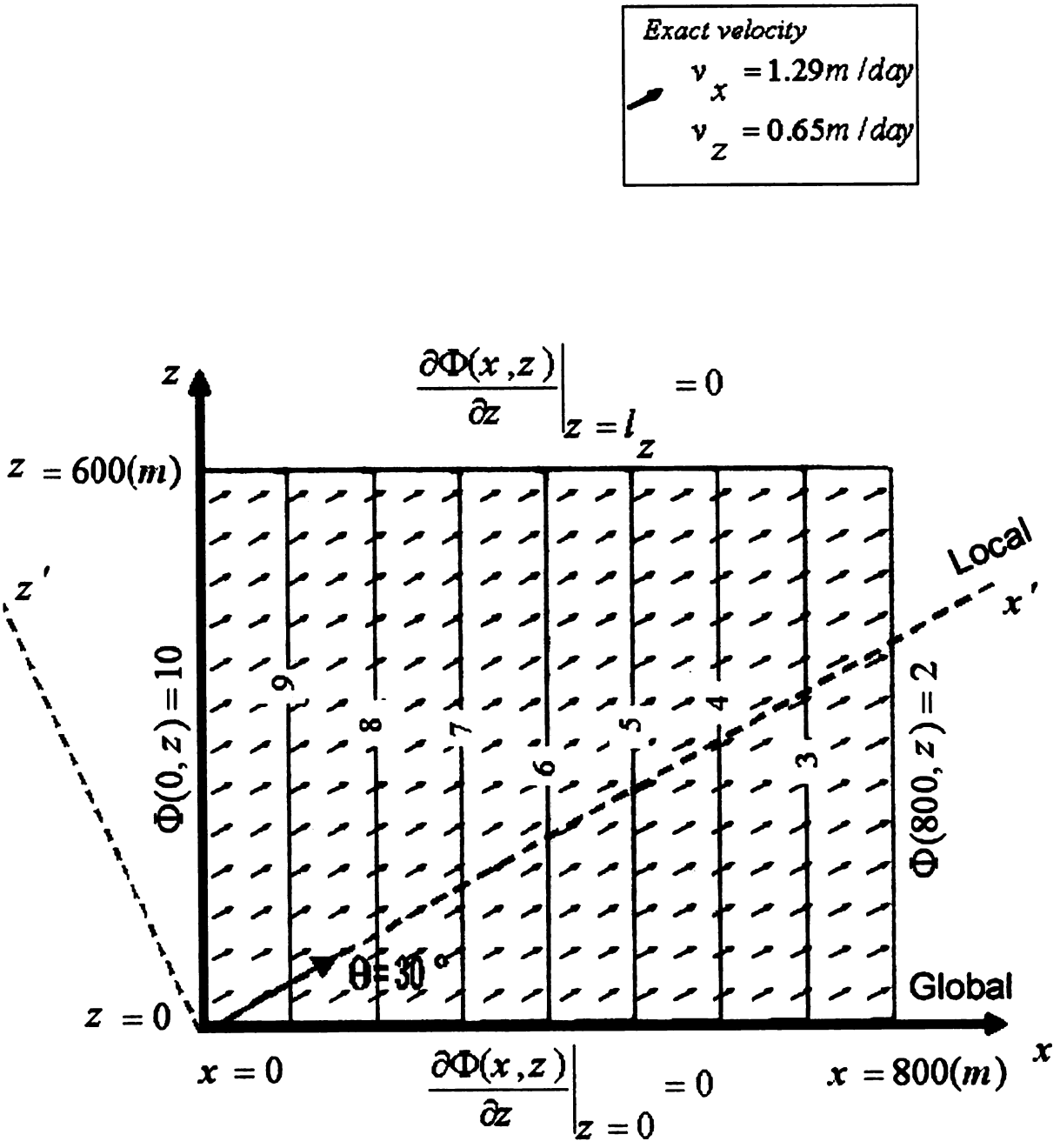

Figure 8. Exact Solution for the simple example.

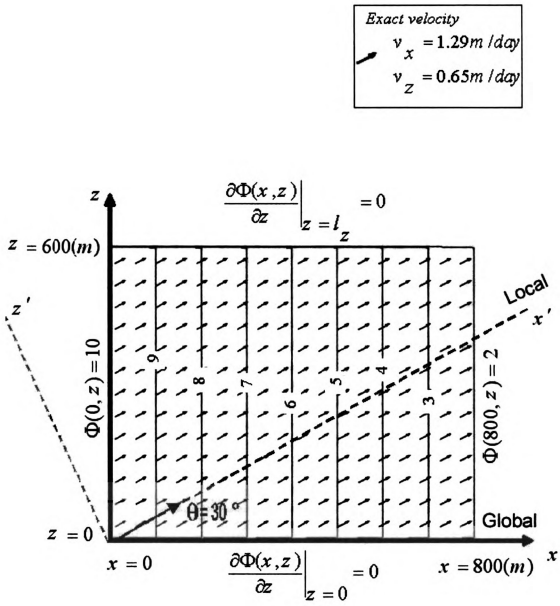

Figure 9. Numerical solution using improved FD method for the simple example.

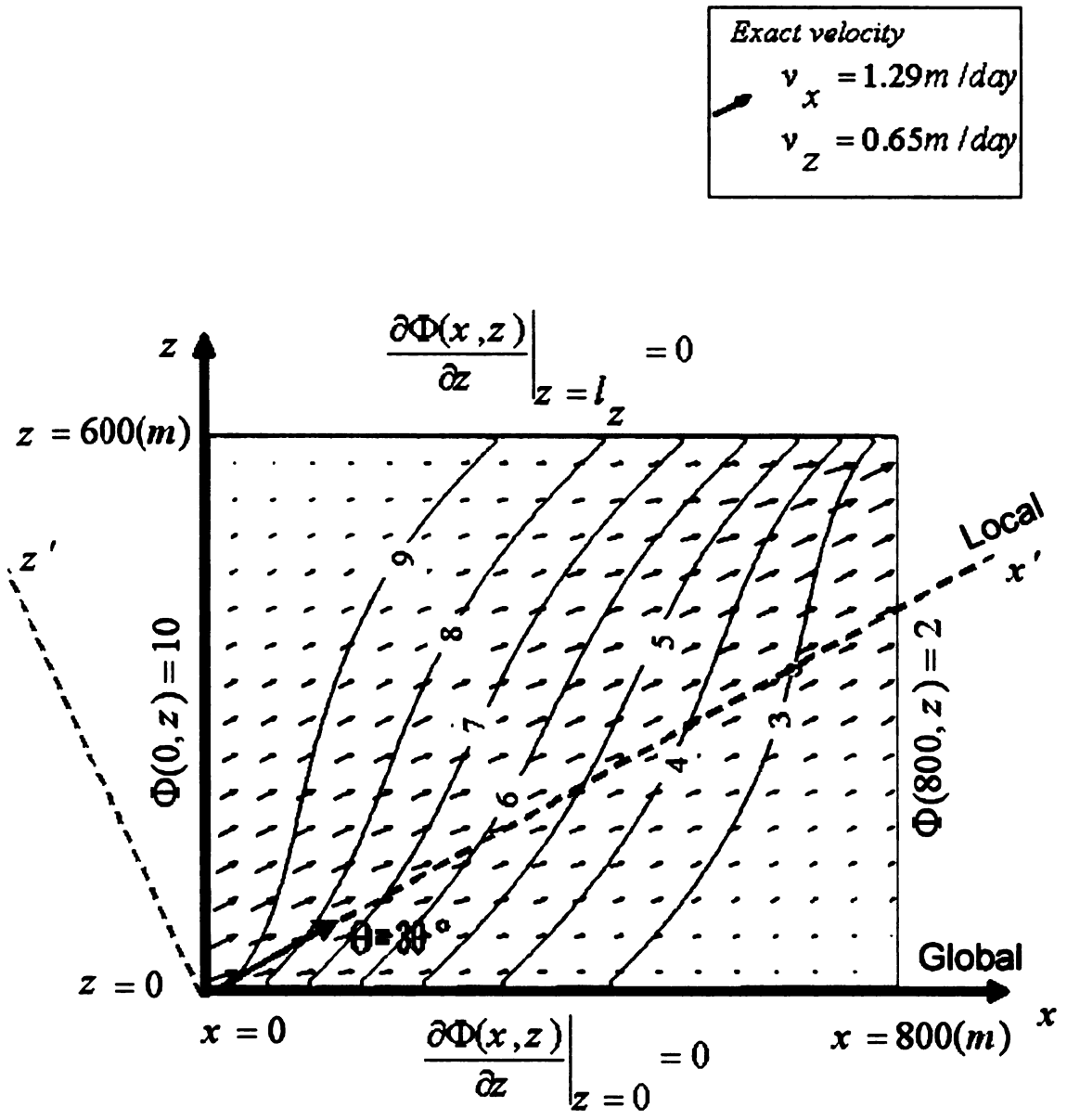

Figure 10. Numerical solution using traditional FD method for the simple example.

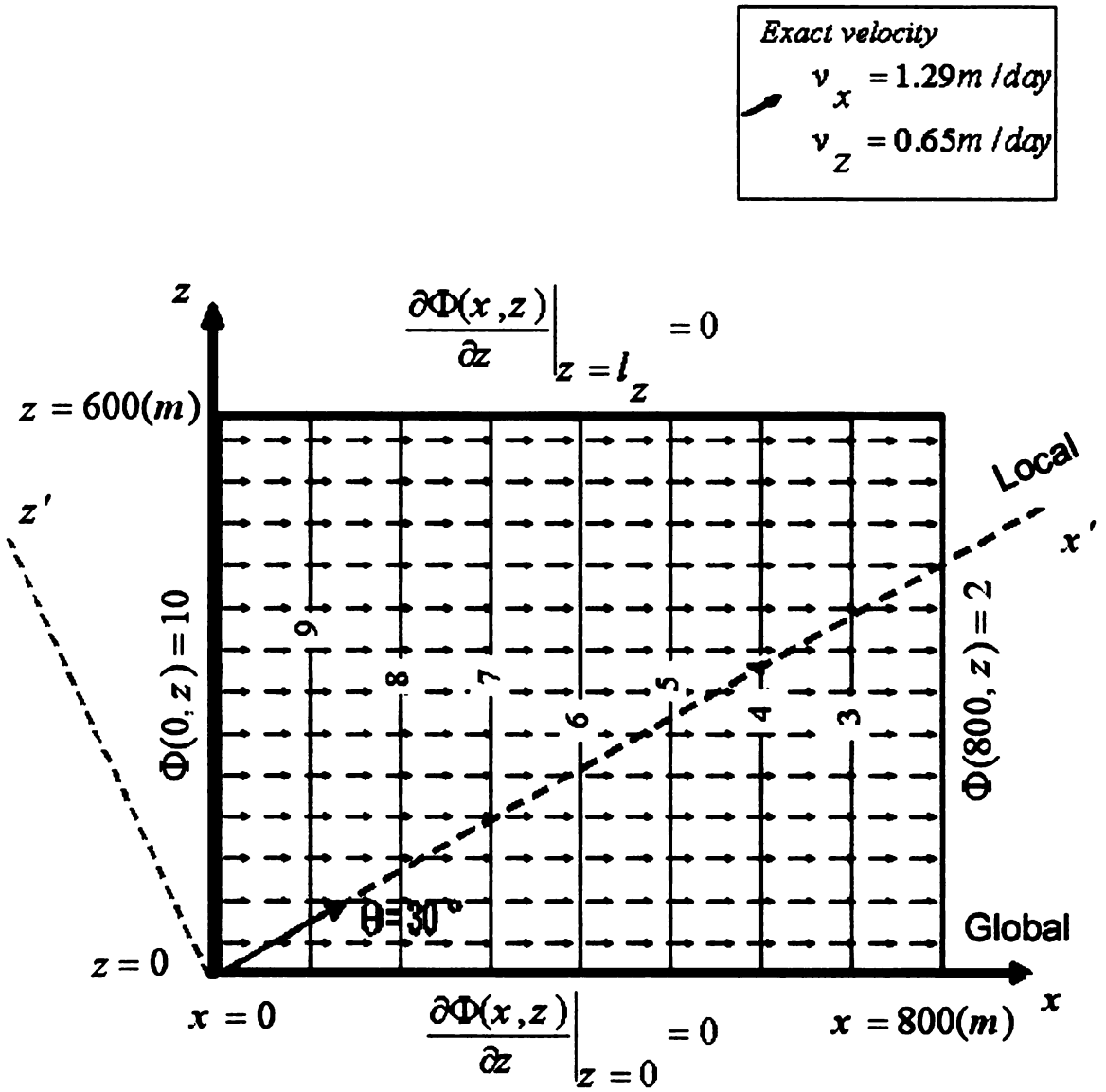

Figure 11. Numerical solution using the MODFLOW approach for the simple example.

We have also tabulated the results in Table 2 for the different methods at three representative points (see Figure 7) to provide a more quantitative comparison.

Table 2 - Comparison of the exact predicted head and velocity at three representative points (Figure 7) with different numerical methods.

Observation point 1

Method	x(m)	z(m)	Φ *(m)*	v_x *(m/day)*	v_z *(m/day)*
Exact	200	63	8	1.29	0.66
Improved	200	63	8	1.29	0.65
Traditional	200	63	6.52	1.1	0.23
MODFLOW	200	63	8	1.67	0

Observation point 2

Method	*x(m)*	*z(m)*	Φ *(m)*	v_x *(m/day)*	v_z *(m/day)*
Exact	402	300	5.98	1.29	0.66
Improved	402	300	5.98	1.29	0.65
Traditional	402	300	5.96	1.21	0.46
MODFLOW	402	300	5.98	1.67	0

Observation point 3

Method	*x(m)*	*z(m)*	Φ *(m)*	v_x *(m/day)*	v_z *(m/day)*
Exact	670	526	3.3	1.29	0.66
Improved	670	526	3.3	1.29	0.65
Traditional	670	526	4.03	1.52	0.48
MODFLOW	670	526	3.3	1.97	0

As shown by Figures 8 through 11 the solution obtained from the improved approach agrees very well with the exact solution. In fact, they are graphically indistinguishable from each other. By contrast, the numerical solution obtained from the traditional FD approach is significantly different from the exact solution for both the predicted heads and velocities. The MODFLOW approach leads to, not surprisingly, wrong velocity direction and magnitude since it ignores the orientation of anisotropy. The additional quantitative comparison in Table 2 leads to the same conclusions.

To further examine why the traditional FD approach, and the MODFLOW approach fail even for such a simple flow situation, we take a close look at basic numerical representation of the various approaches for this simple example. Consider a typical model cell of the discretized domain as shown in Figure 12. As we discussed earlier, the predicted head in a model cell can be expressed as the weighted average of heads in the surrounding cells. The values of the weighting coefficients in this case are shown graphically in the respective cell.

0.0262	0.0192	0.262
0.192		0.192
0.262	0.0192	0.0262

(a) Improved approach

-0.089	0.148	0.089
0.352		0.352
0.089	0.148	-0.089

(b) Traditional approach

0	0.045	0
0.455		0.455
0	0.045	0

(c) MODFLOW approach

Figure 12. Comparison of the weighting coefficients for (a) the improved FD method, (b) the traditional FD method, and(c) the MODFLOW method

As we can see, the weighting coefficients for the improved FD approach (Figure 12a) are all positive and add up to unity. The distribution agrees with what is expected, with the values being an order of magnitude larger in the northeast *(NE)* and southwest *(SW)* cells (along the orientation of anisotropy) than in the northwest *(NW)* and southeast *(SE)*.

In the traditional FD approach, although the weighting coefficients along the orientation still are much larger than those across as they should be, they become negative in the northwest *(NW)* and southeast *(SE)* corner cells. This violates the basic physical principle of groundwater flow since it suggests that an increase in the head in the northwest/southeast *(NW/SE)* cell would cause a decrease in the center head. This wrong hydraulic connection between the central cell and the surrounding cells does not express the natural hydraulic connection between the cells. Misinterpreting the weighting coefficients in a model cell causes the wrong solutions in the traditional FD method (Figure 12b).

In the MODFLOW approach (Figure 12c), all the coefficients are positive but the corner information, which expresses the orientation of anisotropy, is missing. This absence of corner information is what causes the wrong velocity prediction, in the direction and magnitude.

4.2 A More Realistic Example

In this example, we consider a more realistic situation that involves a 2-D vertical flow obtained from a 3-D model slice, in a three-layer aquifer system characterized by highly variable elevations and complex sources and sinks (recharge, surface seepage). The aquifers are assumed to be anisotropic with the bedding oriented along the layers. The ratio of vertical anisotropy is assumed to be the same in all three aquifers. A conceptual sketch, along with the boundary conditions, is provided in Figure 13. The input physical and numerical parameters are provided in Tables 3 and 4.

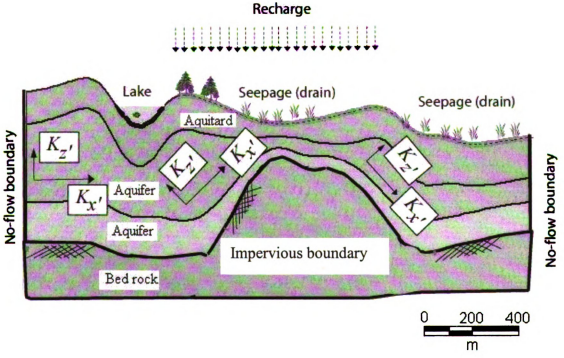

Figure 13. Conceptual sketch with assigned physical and numerical parameters for the realistic example.

Table 3. Physical parameters for three conceptual layers in the realistic example.

Parameter	Value (unit)
θ	*Variable based on geology*
Length of cross section	*2000 (m)*
Width of cross section	*40 (m)*
Depth of cross section	*Variable around 200 (m)*
K_x, *(layer 1)*	*0.05 (m/day)*
K_x, *(layer 2)*	*2 (m/day)*
K_x, *(layer 3)*	*7 (m/day)*
K_z / K_x, *(for each conceptual layer)*	*0.1 (-)*
Recharge (throughout whole domain)	*2.086 E (-3) (m/day)*
Seepage (drain)	*0.005 (1/day)*
River leakance	*5 (1/day)*

Table 4. Input numerical parameters for three conceptual layers in the realistic example.

Input numerical parameters	Value (unit)
Steady state condition	-
Computational layers for each conceptual layer	*2(-)*
Δx	*40 (m)*
Δz	*Variable based on geology (m)*

The problem is solved using both the improved and traditional FD approaches. The results are shown graphically in Figures 14 and 15.

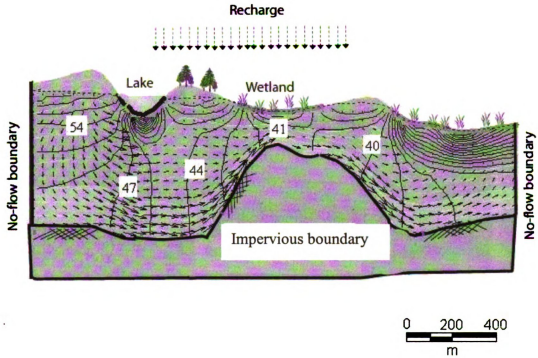

Figure 14. Results of realistic example applying the improved FD approach .

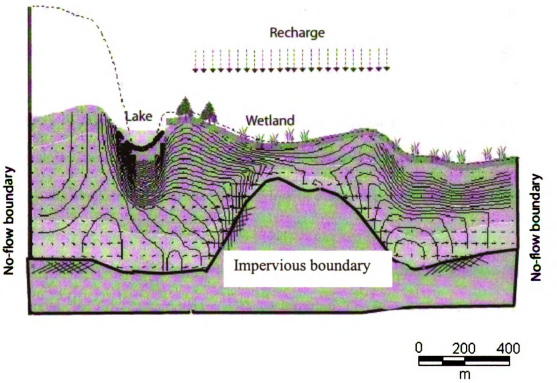

Figure 15. Results of realistic example applying traditional FD approach.

A qualitative comparison of the results obtained from the two different methods reveals clear differences. In fact, the solution from the traditional FD approach (Figure 15) did not even converge and the result is wrong or does not conserve mass. We seemed to frequently have difficulty in obtaining a converged solution with the traditional FD approach whenever the system becomes relatively complex and the number of degree of freedom is large. Even when the solution does converge the rate of convergence is often very slow. These numerical difficulties can all be ultimately attributed to the "negative weighting coefficients" and the resulting loss of diagonal dominance in the matrix systems.

The results show that the improved FD approach leads a meaningful solution (Figure 14). The predicted flow pattern agrees with our intuition. The flow derives from recharge and is drained toward the lake and the wetlands. The solution also shows the impact of the variable anisotropy and the bedrock boundary conditions. In particular, as we expected, the flow follows, to large degree, the orientation of the anisotropy and the shape of the bottom rock. Numerically, the improved approach is robust and always able to produce a converged solution given the boundary conditions and hydrologic stresses.

5 Conclusion

The following conclusion emerge from this thesis:

- Most real-world aquifers are strongly anisotropic. In many cases, the major orientation of the anisotropy varies in space and cannot be aligned with the overall model grid orientation.

- Traditional FD methods that account for the variable orientation are often numerically problematic and lead to inaccurate or physically unrealistic solutions.

- The popular MODFLOW approach is able to circumvent the numerical problem by simply ignoring the orientation of the anisotropy. The resulting solution, though numerically well behaved, is inaccurate, especially in areas where the hydraulic gradient is significantly different the natural orientation of the anisotropy.

- The solution obtained from the improved FD method is significantly more accurate than those obtained from the traditional FD method and the MODFLOW approach. The improved FD method is robust and can adapt to complex flow conditions

Future research should focus on more thorough testing of the improved FD method in three-dimensional (3-D) flow situations.

6 References

Anderman, E.R., and Hill, M.C. (2000). MODFLOW-2000, the U.S. Geological Survey modular ground-water model – Documentation of the Hydrogeologic-Unit Flow (HUF) Package: U.S. Geological Survey Open-File Report 00-342.

Anderman, E.R., Kipp Kenneth L., Hill Marcy C., Valstar Johan, and Neupauer Roseanna M. (2002). MODFLOW-2000, the U.S. Geological Survey modular ground-water model – Documentation of the model-layer variable- irection horizontal anisotropy (LVDA) capability of the Hydrogeologic-Unit Flow (HUF) Package: U.S. Geological Survey Open-File Report 02-409.

Bear, Jacob. (1972). Dynamics of fluid in porous media. New York, American Elsevier.

Dale F. Ritter. (1986). Process geomorphology. Wm.C. Brown Publishers, Dubuque, Iowa.

Dash, Z.V., Zyvoloski, G.A., and Robinson,B.A.. (2002). User's manual for the FEHM application a finite-element heat- and mass-transfer code. Los Alamos, New Mexico, Los Alamos National Laboratory Report LA-13306-M.

Davis, S. N. (1969). Porosity and permeability of natural materials. Flow through porous media. ed. R. J. M. De Wiest. Academic Press, New York.

Harbaugh, A.W., Banta, E.R., Hill, M.C., and McDonald, M.G.. (2000). MODFLOW-2000, the U.S. Geological survey modular ground-water model – User guide to modularization concepts and the ground-water flow process. U.S. Geological Survey Open-File Report 00-92.

Lin, H.-C. J., D.R. Richards, C.A. Talbot, G.-T. Yeh, H.-P. Cheng, N.L. Jones. (2001). FEMWATER: A three-dimensional finite element computer model for simulating density-dependent flow and transport in variably saturated media, Version 3.0. Technical Report CHL-01-***, U.S. Army Engineer Waterways Experiment Station.

Mary P. Anderson, William W. Woessner. (1992). Applied groundwater modeling. Academic Press, Inc.

Massimo Ferraresi, Alberto Marinelli. (1996). An extended formulation of the integrated finite difference method for groundwater flow and transport. Journal of Hydrology. Amsterdam : Elsevier Science B.V. Feb 1996. v.175 (1/4) p. (453-471).

Michael J. Friedel. (2001). A model for simulating transient,variably saturated, coupled water-heat-solute transport in heterogeneous, anisotropic,2-dimensional, ground-water systems with variable fluid density. Water-Resources Investigations Report 00–4105 Urbana, Illinois.

Molson, J.W., and Frind, E.O. (2002). WATFLOW/WTC user guide and documentation. Version 3: Waterloo, Ontario, Canada, Department of Earth Sciences, University of Waterloo.

R.Allan Freeze, John A. Cherry. (1979). Groundwater. Prentice Hall Inc.

Shu-Guang Li. (2002). Interactive groundwater model (IGW). Michigan State University: http://www.egr.msu.edu/~lishug.

Voss, C.I., and Provost, A.M.. (2002). SUTRA - A model for saturated-unsaturated variable-density groundwater flow with solute or energy transport. U.S. Geological Survey Water-Resources Investigations Report 02-4231.

Wang, H.F. and Anderson, M.P.. (1982). Introduction to groundwater modeling, finite difference and finite element methods. San Francisco, W.H Freeman and Company.